This article was downloaded by:
On: *15 January 2011*
Access details: *Access Details: Free Access*
Publisher *Taylor & Francis*
Informa Ltd Registered in England and Wales Registered Number: 1072954 Registered office: Mortimer House, 37-41 Mortimer Street, London W1T 3JH, UK

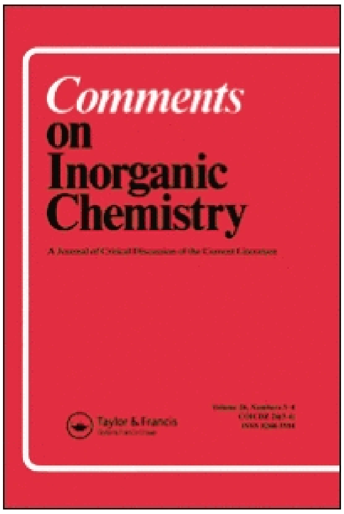

Comments on Inorganic Chemistry

Publication details, including instructions for authors and subscription information:
http://www.informaworld.com/smpp/title~content=t713455155

X-Ray Structural Studies of Adenosine 5'-Triphosphate Metal Compounds

Renzo Cini[a]
[a] Dipartimento di Chimica dell'Università degli Studi di Siena, Siena, Italy

To cite this Article Cini, Renzo(1992) 'X-Ray Structural Studies of Adenosine 5'-Triphosphate Metal Compounds', Comments on Inorganic Chemistry, 13: 1, 1 — 34

To link to this Article: DOI: 10.1080/02603599208048457

URL: http://dx.doi.org/10.1080/02603599208048457

PLEASE SCROLL DOWN FOR ARTICLE

Full terms and conditions of use: http://www.informaworld.com/terms-and-conditions-of-access.pdf

This article may be used for research, teaching and private study purposes. Any substantial or systematic reproduction, re-distribution, re-selling, loan or sub-licensing, systematic supply or distribution in any form to anyone is expressly forbidden.

The publisher does not give any warranty express or implied or make any representation that the contents will be complete or accurate or up to date. The accuracy of any instructions, formulae and drug doses should be independently verified with primary sources. The publisher shall not be liable for any loss, actions, claims, proceedings, demand or costs or damages whatsoever or howsoever caused arising directly or indirectly in connection with or arising out of the use of this material.

X-Ray Structural Studies of Adenosine 5′-Triphosphate Metal Compounds

RENZO CINI
Dipartimento di Chimica
dell'Università degli Studi di Siena,
Pian dei Mantellini 44,
I-53100 Siena, Italy

Received September 10, 1991

Solid state structures of the ATP-metal compounds are critically analyzed. Particular attention is devoted to the metal coordination and its influence on the conformation of the triphosphate chain and ribose ring. The three phosphate groups are involved in the coordination in all the compounds. The strongest coordinating group is γ-phosphate, while α-phosphate is the weakest. The γ-phosphate can coordinate to two metal cations, allowing the formation of dimeric species. The triphosphate chain reveals a high degree of flexibility about its backbone bond and torsion angles; however, it is always in a bent conformation with the P···P···P angle ranging from 85–100°. The O(βγ)–P(γ) bond is the longest of the backbone O–P linkages. The conformation of the ribose ring is commonly C(2′)- or C(3′)-*endo*; however, one ATP molecule has a C(4′)-*endo* geometry. The orientation of the adenine system about the glycosidic linkage is *anti*. The adenine system does not show any donating ability in most of the structures. Nevertheless, formation of a macrochelate through the coordination of adenine N(7) and γ-phosphate oxygen atoms to sodium ions was found in the structures of ATP-disodium salt. Furthermore, the adenine system is involved in *stacking interactions* and in some type of base pairing via H-*bridges* in all the ATP-metal compounds. The presence of an aromatic base facilitates the formation of crystalline material. The base can act as a ligand for the metal cation, or it can just stabilize the crystal lattice via weak interactions such as *stacking forces* and H-*bonds*. Previously unpublished data for $[Co(HATP)_2][Co(H_2O)_6]\cdot 2(HDPA)\cdot 9H_2O$ are reported. The review also includes data relevant to ADP-metal compounds.

Comments Inorg. Chem.
1992, Vol. 13, No. 1, pp. 1–34
Reprints available directly from the publisher
Photocopying permitted by license only

Key Words: *adenosine 5'-triphosphate, ATP, ATP-metal compounds, adenosine 5'-diphosphate, ADP, ADP-metal compounds*

I. INTRODUCTION

It is well known that adenosine 5′-triphosphate (hereafter ATP) is the standard currency in the economics of living cells.[1a,b] It is practically impossible to give an exhaustive report of the works that have appeared in the literature, whose main subjects are the enzymatic reactions on ATP (or its analogues). At least seven papers have appeared in the first 22 issues of Vol. 30 (1991) of Biochemistry on this matter,[1c–i] and at least nine reviews have been published (or are in preparation) in only three selected journals in the last six years.[1j–r] The phosphate units can be hydrolyzed in an enormous number of enzymatic processes to produce adenosine 5′-diphosphate (ADP), or adenosine 5′-monophosphate (AMP); the free energy change drives a variety of biochemical processes or performs mechanical work via muscle contraction.[1a–r] The human body is a large-scale maker and consumer of ATP. It has been estimated that during a fast tennis game an amount of 500 g of ATP per minute per man can be burned, whereas at rest the consumption can be about 40 kg of ATP per day per person.[1s]

All the enzymatic reactions of ATP require the presence of metal ions which interact only with the enzyme molecule or bind ATP to form complex molecules that act as the real substrates. Mg(II)-ATP species often accomplish this role.[1t] Therefore many workers have carried out extensive investigations to elucidate the structure of ATP-metal complexes. Binary M-ATP and ternary M-ATP-L (L = low molecular weight ligand) systems have been widely studied in the solution phase.[1u–x] Furthermore, nucleoside 5′-monophosphate-, nucleoside-, and nucleobase-metal compounds have also been thoroughly investigated to shed light on the importance of metal species in genetic information transfer and on anticancer activity. At least nine reviews published since 1980 describe the results of these studies.[1y–ig] On the other hand, enzyme/M/ATP (or ATP derivative) complexes have been investigated with X-ray diffraction,[1ih–ij] and with a combination of X-ray diffraction and model building.[1ik] However, the literature on X-ray structures of nucleoside 5′-triphosphate-metal compounds has not been described in any review, to my knowledge.

This work reports on the structural studies carried out, with single crystal diffraction techniques, on metal compounds of ATP (the enzyme/M/ATP complexes are not included) to examine in depth the conformation of the nucleotide and its behavior as ligand.

The number of ATP-metal compounds investigated to date is relatively small, the major reason being the difficulties in preparing suitable single crystals. Nevertheless, it seemed important to correlate and to critically analyze the data available and to summarize the most successful synthetic strategies.

To clarify the discussion, all the data reported here are referred to the labelling scheme pictured in Fig. I.1.

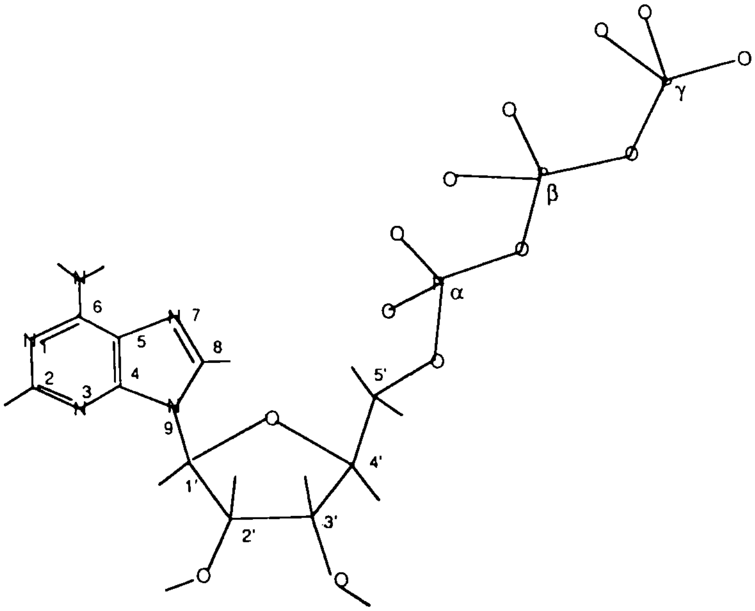

FIGURE I.1 The molecule of ATP^{4-} with the labelling scheme used in this review.

II. ATP-METAL COMPOUNDS

The ATP-metal compounds studied by single crystal X-ray diffraction are reported in Table II.1.

II.1 Synthesis of ATP-Metal Compounds

Crystalline ATP-metal compounds were usually obtained from slightly acidic aqueous solutions of the components. Preparation of single crystals required care, since evaporation of solutions containing metal salts and ATP leaves a mixture of metal phosphate and AMP.

Single crystals of $Na_2H_2ATP \cdot 3H_2O$ were prepared from a water/dioxane solution of the commercial disodium salt by diffusion of dioxane.[2,3] Very thin blades (at best, 0.003 mm thick) with mechanical deformities were obtained.

TABLE II.1

Relevant data for crystalline ATP-metal compounds

Compound	Preparation	Space Group	R_F%[a]	Ref.
$Na_2H_2ATP \cdot 3H_2O$	water/dioxane or water/1-propanol	$P2_12_12_1$	11.7	2–5
$Na_2H_2ATP \cdot 2H_2O$	water/1-propanol	$P2_12_12_1$	9.7	5
$[Zn(H_2ATP)(BIPY)]_2 \cdot 4H_2O$	water, pH 4	$P2_1$	9.8	6–8
$[Cu(H_2ATP)(PHEN)]_2 \cdot 7H_2O$	water, pH 2.8	$P2_1$	6.9	9, 10
$[Mg(HATP)_2][Mg(H_2O)_6] \cdot 2(HDPA) \cdot 12H_2O$	water, pH 5.0	$C222_1$	11.1	11–13
$[Ca(HATP)_2][Ca(H_2O)_6] \cdot 2(HDPA) \cdot 9H_2O$	water, pH 5.0	$C222_1$	12.4	11–13
$[Mn(HATP)_2][Mn(H_2O)_6] \cdot 2(HDPA) \cdot 12H_2O$	water, pH 4.5	$C222_1$	7.2	11, 12, 14
$[Co(HATP)_2][Co(H_2O)_6] \cdot 2(HDPA) \cdot 9H_2O$	water, pH 4.5	$C222_1$	11.1	11, 12, 15
$[Zn(HATP)_2][Mg(H_2O)_6]_{0.72} [Zn(H_2O)_6]_{0.28} \cdot 2(HDPA) \cdot 12H_2O$	water, pH 4.5	$C222_1$	9.0	16
$[Cd(HATP)_2][Ca(H_2O)_6] \cdot 2(HDPA) \cdot 9H_2O$	water, pH 4.5	$C222_1$	10.1	16

[a] When more than one X-ray analysis was carried out, the value of R_F% reported here is the lowest one.

Single crystals of $Na_2H_2ATP \cdot 2H_2O$ were grown from water/1-propanol (1:2.5 v/v) solution by slow evaporation, at room temperature.[5a] The crystals had the shape of thin plates (approximately 0.01 mm thick); the water content increased up to $Na_2H_2ATP \cdot 3H_2O$ as the relative humidity of the surroundings was increased from 5% to 50% at 23°C.[5a]

Crystalline powders of the $[M(H_2ATP)(BIPY)]_2 \cdot 4H_2O$ compounds[8] (M = Mn(II), Co(II), Cu(II), Zn(II), BIPY = 2,2'-bipyridyl, Fig. II.1.1) were obtained from ethanol/water solutions of BIPY, commercial Na_2H_2ATP and the metal sulfate in a 1:1:1 molar ratio.

Single crystals of $[Zn(H_2ATP)(BIPY)]_2 \cdot 4H_2O$[7] were prepared by slow evaporation of very dilute ethanol/water solutions adjusted to pH 4 by adding H_2SO_4. The crystals that formed exhibited large deformities.

Single crystals of $[Cu(H_2ATP)(PHEN)]_2 \cdot 7H_2O$[10] (PHEN = 1,10-phenanthroline, Fig. II.1.1) were prepared by adding a mixture of copper nitrate, PHEN and water to an aqueous solution of Na_2H_2ATP. The components were in a 1:1:1 molar ratio. The initial pH was adjusted at 2.8. The solution was heated up to 80°C for 30 min and then allowed to cool and evaporate at room temperature. The crystal used for data collection had suitable dimen-

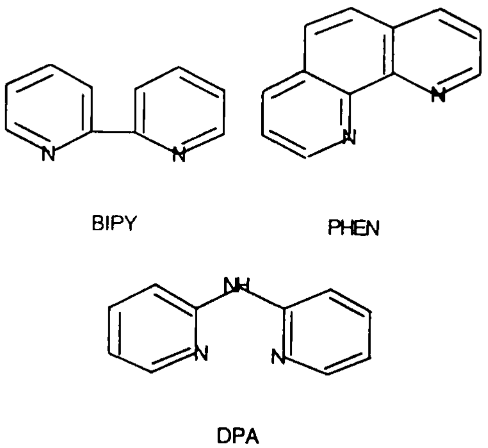

BIPY

PHEN

DPA

FIGURE II.1.1 The aromatic bases of some ATP-metal compounds.

sions. The agreement R index converged down to 6.9,[10] the lowest value so far reported for the ATP-metal compounds.

Crystalline powders of the $[M(HATP)_2][M(H_2O)_6] \cdot 2(HDPA)$ nH_2O (M = Mg(II), Ca(II), Mn(II) and Co(II), DPA = bis(2-pyridyl)amine, Fig. II.1.1) compounds[11-13] were obtained by following a procedure similar to that used for the $[M(H_2ATP)(BIPY)]_2 \cdot 4H_2O$[8] compounds. The pH of the mother liquor ranged from 4.2 to 5.4, depending on the metal ion.

Single crystals were obtained by slow cooling of hot dilute aqueous solutions.[13] The Mg(II) and Ca(II) derivatives grew as needles showing large cracks. The Co(II) derivative produced pink prisms with large mechanical deformities. The Mn(II) compound produced good quality prisms which allowed refinement of the structure to a final agreement index R of 7.2,[14] even though the $HDPA^+$ molecules were affected by statistical disorder. The H atoms could be located from the difference Fourier synthesis. The atomic coordinates show the lowest estimated standard deviations so far reported for ATP-metal compounds.

Crystalline powders and single crystals of the $[M_{1-p}M'_p(HATP)_2]$ $[M_{1-q}M'_q(H_2O)_6] \cdot 2(HDPA) \cdot nH_2O$ mixed metal complexes with a variable overall M/M′ molar ratio, which depends on the composition of the mother liquor, were obtained from water/ethanol solution.[16] Each M-M′ couple gave a series of complexes that differ from each other in the overall M/M′ ratio. A systematic investigation of the relationship between the M/M′ molar ratio in the mother liquor and in the solid state was carried out for the series: Mg(II)/Mn(II), Mg(II)/Fe(II), Mg(II)/Co(II), Mg(II)/Zn(II), Mg(II)/Cd(II), Ca(II)/Mn(II) and Ca(II)/Cd(II). The M/M′ molar ratio in the mother liquor was varied over a wide range for most of the systems. Crystalline products were usually obtained. However, single crystals from the Ca(II)/Cd/ATP/DPA system could be prepared only when the Ca/Cd ratio in the starting mixture was 1.

II.2 The Triphosphate Chain

The most active donating moiety of ATP is the triphosphate chain. As the metal coordination has some influence on the chain conformation, the two structural aspects will be treated together. The ATP-metal complexes show analogies and differences in the chain structure. The most evident analogy is that of the folded conformation with the P···P···P angle included in the range 85–100°. This geometry facilitates a facial coordination of the negatively charged phosphate groups to the metal cation.

The two molecules of the dimer of $Na_2H_2ATP \cdot 3H_2O^2$ are reported in Fig. II.2.1. Oxygen atoms from the α-, β- and γ-phosphate groups are linked to the metal ions. However, the triphosphate chains of each dimer are tightly bound to only one type of sodium ion (two ions). The Na-O_α, -O_β and -O_γ bond distances range from 2.38(2) to 2.55(2) Å, are 2.44(2) Å, and range from 2.33(2) to 2.63(2) Å, respectively, for $Na_2H_2ATP \cdot 3H_2O$.[5a] A second group of two sodium ions is coordinated by both phosphate oxygen atoms (only O_α and O_β) and water molecules. In this case, the Na-O_α and -O_β distances are 2.62(4), and 2.36(2) and 2.42(2) Å, respectively, for $Na_2H_2ATP \cdot 3H_2O$.[5a] The coordination scheme around the first group of sodium ions of $Na_2H_2ATP \cdot 2H_2O^{5a}$ is

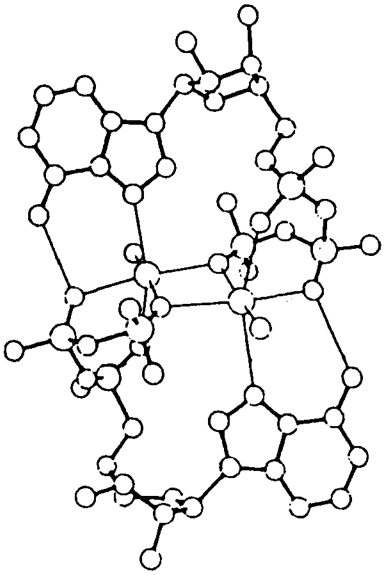

FIGURE II.2.1 Dimer of $Na_2H_2ATP \cdot 3H_2O$. The coordination bonding to the Na^+ ions and H-*bonds* involving NH_2 adenine groups are shown. Octahedral geometry around each Na^+ ion is completed by a γ-phosphate oxygen atom from translated dimer (from Ref. 2, with permission).

similar to that of the trihydrate form. On the other hand, some differences in the coordination scheme of the second type of sodium ions occur on changing the number of water molecules. The triphosphate chains point towards the adenine bases. However, the P atoms are not coplanar with the base atoms. The folding of the chain is stabilized by the sodium ions that bridge the N(7) atoms and the γ-phosphate groups.

The bent conformation of triphosphate was observed also for $[Zn(H_2ATP)(BIPY)]_2 \cdot 4H_2O$[7] (Fig. II.2.2) and $[Cu(H_2ATP)(PHEN)]_2 \cdot 7H_2O$[10] (Fig. II.2.3), for which the P···P···P angles are 94(2) and 87(2)°, and 93.5(3) and 88.8(3)° for the two molecules of the dimers, respectively. The nitrogen atoms of BIPY and PHEN exclude the N(7) atom from the coordination sphere. This explains the lack of folding in the triphosphate chain towards the adenine system.

Metal coordination to the γ- and β-phosphate groups is strong for both $[Zn(H_2ATP)(BIPY)]_2 \cdot 4H_2O$[7] and $[Cu(H_2ATP)(PHEN)]_2 \cdot 7H_2O$[10] dimers. The Zn-O(γ) and Zn-O(β) bond distances average 2.03(3) Å. On the other hand, the Zn-O(α) bond distances are 2.71(4) and 2.39(3) Å for the two molecules of the dimer,

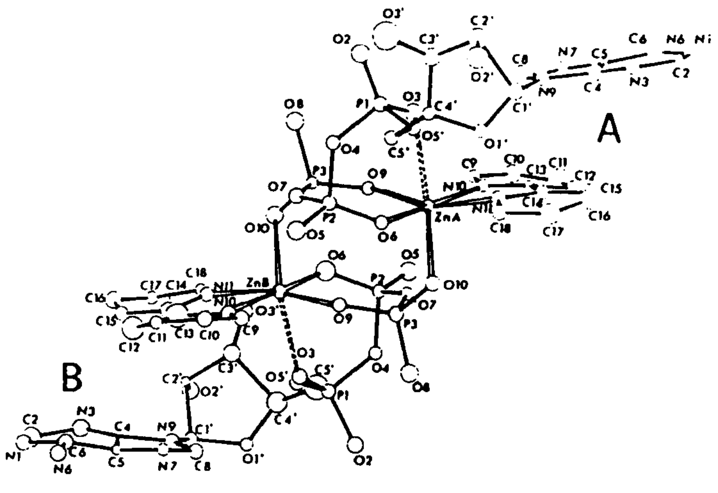

FIGURE II.2.2 ORTEP drawing of the $[Zn(H_2ATP)(BIPY)]_2$ dimer (from Ref. 7).

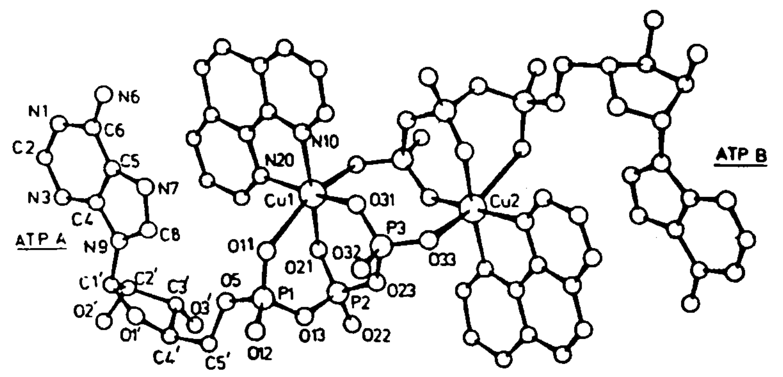

FIGURE II.2.3 View of the $[Cu(H_2ATP)(PHEN)]_2$ dimer (from Ref. 10, with permission).

respectively. Distorted octahedral coordination geometries are found in a variety of Zn(II) complexes.[17,18]

The long Zn-O(α) bond distance found in one moiety of $[Zn(H_2ATP)(BIPY)]_2 \cdot 4H_2O$[7] dimer can be related to the intramolecular *stacking interactions* and intermolecular *H-bonds*. It is supposed that the strongest adenine··· BIPY interaction can assist the shift of an O(α) atom away from the Zn center. Furthermore, the strong intermolecular *H-bonds* involving a O(α) atom and a NH_2 group contribute to the difference in the Zn-O(α) bond lengths.

The Cu-O(β) and Cu-O(γ) bond distances relevant to the same ATP molecule of $[Cu(H_2ATP)(PHEN)]_2 \cdot 7H_2O$[10] average 1.941(9) Å. However, both the Cu-O(γ) linkages that bridge the two moieties of the dimer are longer than the other Cu-O(γ) bonds and average 2.279(8) Å. The two Cu-O(α) bond distances are: 2.878(9) and 2.730(9) Å. If the equatorial planes are considered to be defined by the two nitrogen atoms from PHEN and the O(β) and O(γ) donors from the same triphosphate chain, the $[Cu(H_2ATP)(PHEN)]_2 \cdot 7H_2O$[10] compound shows the usual axially elongated coordination geometry.[19]

The series of $[M(HATP)_2][M_{1-q}M'_q(H_2O)_6] \cdot 2(HDPA) \cdot nH_2O$ compounds[13-16] shows a folded triphosphate chain, too; the P··· P··· P angle being 85(1), 87(1), 86.0(5), 85(1), 85.1(7), and 86(1)° for the $q = 0$, M = Mg(II), Ca(II), Mn(II), Co(II), and $q = 0.72$, M = Zn(II), M′ = Mg(II), and $q = 1$, M = Cd(II), M′ = Ca(II)

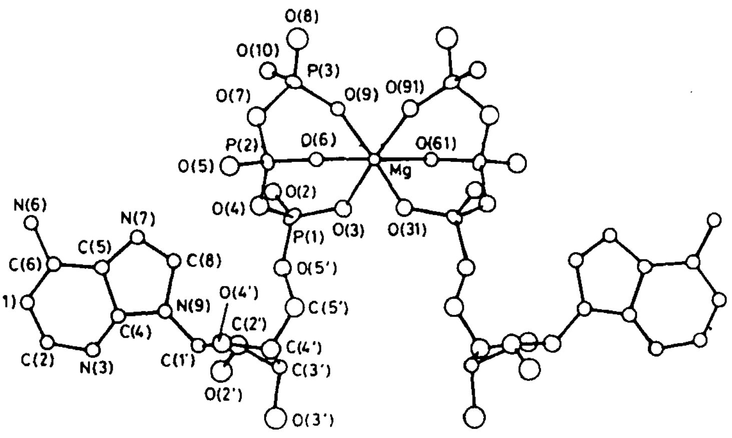

FIGURE II.2.4 ORTEP drawing of the [Mg(HATP)$_2$]$^{4-}$ complex (from Ref. 13).

derivatives, respectively (Fig. II.2.4). Both alkaline-earth (Mg(II) and Ca(II)) and some *d-block* divalent cations (Mn(II), Co(II), Zn(II) and Cd(II)) are linked to six oxygen atoms from the phosphate groups of two ATP molecules without any bonding interaction to the HDPA$^+$ base.

Some interesting points about the triphosphate chain conformation for the [M(HATP)$_2$]$^{4-}$ complexes[13-16] must be emphasized:

(a) The chain points away from the adenine base (see below Table II.2.3 for the C(4')-C(5')-O(5')-P(α) and O(5')-P(α)-O-P(β) torsion angles, and Fig. II.2.4).

(b) All the metal ions coordinate more strongly to the O(γ) oxygen atom than to the O(β) and O(α) ones. The M-O bond length usually increases in the order M-O(γ) < M-O(β) < M-O(α). However, the M-O(α) interaction is stronger for the [M(HATP)$_2$]$^{4-}$ species[13-16] than for the [Zn(H$_2$ATP)(BIPY)]$_2\cdot$4H$_2$O[7] and [Cu(H$_2$ATP)(PHEN)]$_2\cdot$7H$_2$O[10] compounds, when compared to the M-O(β) and M-O(γ) ones.

(c) The triphosphate chain interacts with hydrated metal cations via a network of *H-bonds* involving chiefly the γ-phosphate group.

The average backbone P-O bond distances for all the compounds are reported in Table II.2.1. It should be pointed out that the mean O(βγ)-P(γ) bond length is the longest backbone P-O bond distance. The mean of all the P(γ)-O(p) bond lengths is 1.482 Å, while the ideal P-O bond distance is 1.54 Å for the PO_4^{3-} group,[20] and the mean P-O distance calculated from 45 structures of inorganic salt and other compounds is 1.546 Å.[20]

The C(5′)-O(5′)-P(α) angle ranges from 113 to 128°, in agreement with some double bond character for the P-O ester linkage (ideal P-O single bond distance = 1.71 Å[20]; ideal P = O double bond distance = 1.40 Å[20]; mean O(5′)-P bond distance for the ATP-metal compounds 1.56 Å, Table II.2.1).

The P-O-P backbone bond angles are reported in Table II.2.2. The P(α)-O-P(β) and P(β)-O-P(γ) bond angles range from 127 to 139° and show a tendency towards a linear relationship to the metal ionic radius. This is most remarkable when the comparison involves the $[M(HATP)_2]^{4-}$ compounds, for which the packing forces should be similar. The smallest divalent cation, namely Mg(II), causes the narrowest P-O-P angles for all the ATP complexes. The (C/P)O-P-O(P) bond angles are not much influenced by the nature of the cation. They range from 99 to 108°.

The values of the backbone torsion angles (Table II.2.3) reveal a high pliancy of the triphosphate chain. The differences found for the torsion angles of $Na_2H_2ATP \cdot 3H_2O$[5a] and $Na_2H_2ATP \cdot 2H_2O$[5a] are noteworthy. The C(4′)-C(5′)-O(5′)-P(α) torsion angles show large deviations from the *trans* conformation for $Na_2H_2ATP \cdot 3H_2O$, $[Zn(H_2ATP)(BIPY)]_2 \cdot 4H_2O$ and one of the ATP molecules of $[Cu(H_2ATP)(PHEN)]_2 \cdot 7H_2O$. These deviations do not usually occur for nucleoside 5′-monophosphates, while they are considered

TABLE II.2.1

Mean backbone P-O bond length (Å) for the ATP-metal compounds. The mean of the peripheral P(γ)-O(p) and -O(p)H bond distances for $Na_2H_2ATP \cdot 3H_2O$, $Na_2H_2ATP \cdot 2H_2O$, $[Cu(H_2ATP)(PHEN)]_2$ and $[Mn(HATP)_2]^{4-}$ species are also reported

O(5′)-P(α)	P(α)-O(αβ)	O(αβ)-P(β)	P(β)-O(βγ)	O(βγ)-P(γ)	P(γ)-O(p)	P(γ)-O(p)H
1.560	1.608	1.595	1.589	1.621	1.482	1.542

TABLE II.2.2

Selected backbone bond angles (°) of the triphosphate chain for the ATP-metal compounds. The ionic radius (*Ir* (Å), coordination number = 6)[21] for each metal cation is also reported

Complex	P(α)-O(αβ)-P(β)	P(β)-O(βγ)-P(γ)	*Ir*
$[Mg(HATP)_2]^{4-}$	125(1)	127(1)	0.72
$[Cu(H_2ATP)(PHEN)]_2$	131(1)	130(1)	0.73
	130(1)	131(1)	
$[Co(HATP)_2]^{4-}$	129(2)	129(1)	0.74
$[Zn(H_2ATP)(BIPY)]_2$	130(2)	133(2)	0.75
	127(2)	138(2)	
$[Zn(HATP)_2]^{4-}$	128.4(6)	130.3(6)	
$[Mn(HATP)_2]^{4-}$	130.4(4)	131.1(3)	0.82
$[Cd(HATP)_2]^{4-}$	132.3(8)	132.0(6)	0.95
$[Ca(HATP)_2]^{4-}$	131(2)	132(1)	1.0
$Na_2H_2ATP\cdot 3H_2O$	134(1)	139(1)	1.02
	132(1)	134(1)	
$Na_2H_2ATP\cdot 2H_2O$	133(1)	135(1)	
	137(1)	136(1)	

TABLE II.2.3

Selected torsion angles (°) for the triphosphate chain of some ATP-metal complexes

Complex	C(4′)-C(5′)-O(5′)-P(α)	C(5′)-O(5′)-P(α)-O(αβ)	O(5′)-P(α)-O-P(β)	P(α)-O-P(β)-O(βγ)	O(αβ)-P(β)-O-P(γ)
$Na_2H_2ATP\cdot 3H2O$	−139(1)	72(1)	152(1)	−117(1)	88(1)
	−141(1)	−45(1)	−76(1)	62(1)	−118(1)
$Na_2H_2ATP\cdot 2H_2O$	−146(1)	67(1)	105(1)	−72(1)	127(1)
	−158(1)	75(1)	−119(1)	82(1)	−126(1)
$[Cu(H_2ATP)(BIPY)]_2$	−147(1)	−55(1)	−71(1)	−109(1)	77(1)
	170(1)	72(1)	85(1)	99(1)	−75(1)
$[Mn(HATP)_2]^{4-}$	171(1)	−66(1)	161(1)	64(1)	−100(1)

normal for di- and poly-phosphates for which the base···phosphate attractive interaction can fold the phosphate chain towards the adenine base.[22] However, the conformation around this angle is $+ap^{20}$ for all the $[M(HATP)_2]^{4-}$ complexes.

The conformation around the O(5′)-P(α) bond is +*sc* or −*sc* for all the complexes. The conformation around the P(α)-O(αβ) bond is +*ap* for all the $[M(HATP)_2]^{4-}$ complexes and for one of the ATP molecules of the dimers of the forms of the disodium salt. For the other ATP molecules it is +*sc*, −*sc*, +*ac* or −*ac*. The conformation around the O(αβ)-P(β) bond is +*sc* for all the $[M(HATP)_2]^{4-}$ complexes. It is −*ac* for one of the ATP molecules of the $Na_2H_2ATP \cdot 3H_2O$ and $[Cu(H_2ATP)(BIPY)]_2 \cdot 7H_2O$ dimeric structures, while it is +*sc*, −*sc* or +*ac* for the other one. Finally the conformation around the P(β)-O(βγ) bond is −*ac* for the $[M(HATP)_2]^{4-}$ complexes, and it is +*ac*, −*ac*, −*sc* and +*sc* for the other compounds.

II.3 Chelate Ring Conformation and Chirality of Coordination

The average Q_T^{23} value for the α/β and β/γ rings is 0.65 and 0.29, respectively, for $[Cu(H_2ATP)(PHEN)]_2 \cdot 7H_2O$,[10] showing that the β/γ rings are flatter than the α/β ones. The α/β and β/γ chelate rings of the $[M(HATP)_2]^{4-}$ ions[13-16] have a chair and a skew boat conformation, respectively. The α/β rings are flatter (mean Q_T = 0.49) than the β/γ ones (mean Q_T = 0.59).

The handedness of $[Cu(H_2ATP)(PHEN)]_2 \cdot 7H_2O$[10] is Δ-*exo*[24] for one molecule and Λ-*exo* for the other. The enantiomers of the $[M(HATP)_2]^{4-}$ ions[13-16] can be designated as Λ-*exo*.

II.4 The Ribose Group

The bond distances and bond angles for the ribose moiety may differ slightly, although significantly, depending on the conformation of the sugar ring.[25] However, analysis of the geometrical parameters should be possible only for $Na_2H_2ATP \cdot 2H_2O$,[5a] $[Cu(H_2ATP)(PHEN)]_2$,[10] and $[Mn(HATP)_2]^{4-}$ [14] owing to the high estimated standard deviations for the other species. The C(4′)-O(4′) bond is longer than the C(1′)-O(4′) bond (difference = 7.75 σ, for the manganese complex). This effect was previously noted in Ref. 25a.

The parameters that define the ribose ring conformation are pictured in Fig. II.4.1 and (some of them) reported in Table II.4.1.

The conformation of the ribose ring is usually the common C(2′)-*endo* or C(3′)-*endo*. However, it must be emphasized that molecule B of $Na_2H_2ATP \cdot 2H_2O$[5a] has the rather uncommon C(4′)-*endo* conformation. The degree of pucker, τ_M,[20] is lower for the $[M(HATP)_2]^{4-}$ complexes than for the other species.

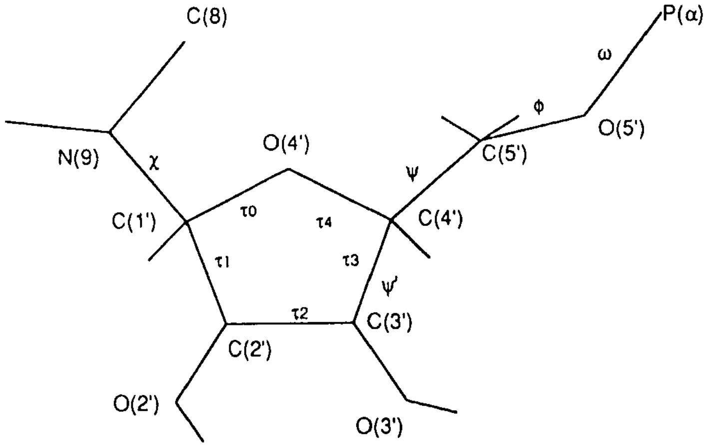

χ	C(8)-N(9)-C(1')-O(4')	ψ_{oc}	C(3')-C(4')-C(5')-O(5')
τ_0	C(4')-O(4')-C(1')-C(2')	ψ_{oo}	O(4')-C(4')-C(5')-O(5')
τ_1	O(4')-C(1')-C(2')-C(3')	ψ'	C(5')-C(4')-C(3')-O(3')
τ_2	C(1')-C(2')-C(3')-C(4')	ϕ	C(4')-C(5')-O(5')-P(α)
τ_3	C(2')-C(3')-C(4')-O(4')	ω	C(5')-O(5')-P(α)-O(αβ)
τ_4	C(3')-C(4')-O(4')-C(1')		

FIGURE II.4.1 Parameters defining the ribose conformation.

The conformation around C(4')–C(5') can be described as *gauche*$^{+}$ [20] for all the ATP-metal compounds, except molecule B of $Na_2H_2ATP \cdot 3H_2O$,[5a] which shows a *gauche*$^{-}$ conformation (ψ_{oc} = $-67°$). As noted in Ref. 5a, the *gauche*$^{-}$ form of the ψ_{oc} torsion angle is necessary for the C(4')-*endo* conformation to avoid contact between C(8) and O(5').

A molecular mechanics investigation has been carried out to investigate the conformational space around the C(4')–C(5') bond. The computations were performed with the MacroModel V3.0 package.[26] The Amber force field[27] was used and the total strain energy of the H_2ATP^{2-} molecule was computed as a function of rotation (step 10°) around ψ_{oc} torsion angle. The strain energy was computed as the sum of the torsion angle deformation, non-bonding interaction, electrostatic interaction, and hydrogen bond interaction contributions. Bond lengths and valence angles were con-

TABLE II.4.1

Phase angle of pseudorotation of the ribose (P) and main torsion angles (°) for some ATP-metal complexes. The ϕ and ω angles are reported in Table II.2.3 (for the Na(I), Cu(II) and M(II) derivatives)

Complex	χ	ψ_{oc}	Conf.	P[a]
$Na_2H_2ATP \cdot 3H_2O$	64(2)	56(2)	C(3′)-*endo*	5
	29(2)	57(2)	C(2′)-*endo*- -C(3′)-*exo*	177
$Na_2H_2ATP \cdot 2H_2O$	61(1)	60(1)	C(3′)-*endo*	11
	4(1)	−67(1)	C(4′)-*endo*	233
$[Cu(H_2ATP)(PHEN)]_2$	32(2)	60(2)	C(3′)-*endo*	16
	6(2)	50(1)	C(3′)-*endo*	15
$[Mn(HATP)_2]^{4-}$	66(1)	55(1)	C(2′)-*endo*- -C(3′)-*exo*	179
$[Co(HATP)_2]^{4-}$	57(3)	60(3)	C(2′)-*endo*- -C(3′)-*exo*	177

[a] The values of P have been calculated on the basis of the equation reported in Ref. 20, without any smoothing of the experimental errors.

strained. The starting structure of $HATP^{3-}$ was that found in the $[Mg(HATP)_2]^{4-}$ complex.[13] A H-atom was added to the γ-phosphate. The absolute minimum occurs at ψ_{OC} and ψ_{OO} of +54° and −63°, respectively. The energy differences between the two relative and the absolute minima are 12 and 8 kJ · mol^{-1}, respectively, while the barriers between the absolute minimum and the relative minima are 23 and 26 kJ · mol^{-1}, respectively. These data are in agreement with the values of ψ_{OO} and ψ_{OC} found for the ATP-metal compounds in the solid state.

The conformation of the glycosidic bond χ is not free but depends on steric hindrance and weak interactions such as *stacking forces* and H-*bonds*. A relationship of χ vs. the C(2′)/C(3′)-*endo* conformation of the ribose was previously noted.[2,20,25b,25c] The χ value is usually larger for a C(2′)-*endo* than for a C(3′)-*endo* sugar conformation.[2]

The C(3′)-*endo* ribose shows a χ torsion angle of 64(2)°, while the C(2′)-*endo*/C(3′)-*exo* sugar has a χ angle of 29(2)° for the $Na_2H_2ATP \cdot 3H_2O$[5a] species. This anomaly was accounted for on the basis of the larger displacement of C(1′B) than that of C(1′A) from the respective adenine system.[2] The χ value for the ATP molecule (B) of $Na_2H_2ATP \cdot 2H_2O$,[5a] which shows a C(4′)-*endo* conformation, is relatively low (4(1)°). As already reported, quantum mechanical calculations give an explanation for these data (see Ref. 5a and references therein).

In $[Zn(H_2ATP)(BIPY)]_2 \cdot 4H_2O$,[7] the two ribose rings have a C(3′)-*endo* conformation. The two nucleosides show a significant difference in the χ angle values (38(3) and −8(3)°, respectively). This difference can be due to different packing forces such as *stacking interactions* and H-*bonds* involving the adenine and the sugar system. A similar trend for the χ value was found for the $[Cu(H_2ATP)(PHEN)]_2 \cdot 7H_2O$[10] compound (see Table II.4.1).

The $[M(HATP)_2]^{4-}$ ions[13–16] show χ values of 67(2), 58(3), 66(1), 57(3), 65(1), 67(2)°, for M = Mg(II), Ca(II), Mn(II), Co(II), Zn(II), Cd(II) respectively, while the conformation of the ribose is C(2′)-*endo*/C(3′)-*exo*.

II.5 The Adenine Group

The N(7) atoms link the Na^+ ions that bridge the adenine systems to the triphosphate chains of the two moieties of the $Na_2H_2ATP \cdot 3H_2O$[5a] and $Na_2H_2ATP \cdot 2H_2O$[5a] dimers. The N(7)–Na internuclear distances are 2.81(1) and 2.59(2) Å, and 2.69(2) and 2.52(2) Å for the trihydrate and dihydrate form, respectively. It should be noted that the ionic radius for hexa-coordinated Na^+ ions is 1.02 Å,[21] while the van der Waals radius for N is 1.55 Å.[28] The NH_2 and N(1)–H groups are involved in the H-*bond* network.

No inner-/outer-sphere coordination to the zinc ions involves the nitrogen atoms of the adenine systems of $[Zn(H_2ATP)(BIPY)]_2 \cdot 4H_2O$.[7] The C(6)–$NH_2$ bond distances average 1.30(4) Å, suggesting a double-bond character. The NH_2 groups are involved in the H-*bond* scheme. The analysis of the H-*bridges* suggests that the NH_2 groups are almost coplanar with the adenine system and that both the N(1) atoms are protonated.

The N(9)–C(1′) bond distances average 1.48(1) Å for the $[Cu(H_2ATP)(PHEN)]_2 \cdot 7H_2O$[10] complex. The C(1′) and N(3) atoms of a molecule interact via a H-*bond*.[28–30] In fact, the C(1′)···N(3) distance and the C(1′)–H(1′)···N(3) angle are 3.06 Å and 95(2)°, respectively. The C(6)–NH_2 average distance (1.31(2) Å) is consistent with a percentage of double bond character. The atoms of each adenine system are almost planar. The C(6)–N(1)–

C(2) angle averages 123(1)°, in agreement with the protonation on N(1) on the basis of the empirical Singh rule,[31] which states that the C(2)–N(1)–C(6) angle is in the range 125 ± 3° if N(1) is protonated, and 116 ± 3° if there is no proton on N(1).

The N(9)–C(1′) bond length is 1.47(1) Å for $[Mn(HATP)_2]^{4-}$.[14] The H(1′) atom, located from the analysis of the experimental X-ray data for the Mn(II)[14] derivative, is involved in the N(3)···C(1′) H-*bond* interaction, the N(3)···C(1′) distance and C(1′)–H···N(3) angle being 3.05 Å and 110°, respectively. The C(2)–N(1)–C(6) bond angle is 117(2), 119(3), 123(1), 118(2), 121(1) and 120(1)° for the $[M(HATP)_2]^{4-}$ complexes with M = Mg(II),[13] Ca(II),[13] Mn(II),[14] Co(II),[15] Zn(II),[16] and Cd(II),[16] respectively.

The N(1) atom turns out to be the only protonated site in $[Mn(HATP)_2]^{4-}$, as clearly revealed by the X-ray analysis. Owing to the isomorphism of crystals of the Mg(II), Ca(II), Co(II), Zn(II), Cd(II) and $[Mn(HATP)_2]^{4-}$ ions, it seems reasonable to conclude that N(1) is protonated for all the species. However, it must be noted that the value of the C(2)–N(1)–C(6) bond angle for the Mg(II), Ca(II) and Co(II) derivatives, indicates that the N(1) atom is not protonated, on the basis of the Singh rule. On the other hand, the relatively high estimated standard deviations preclude a sure conclusion for these three species. However, the intermolecular H-*bond* interaction between N(1) and a γ-phosphate oxygen atom, found for all the $[M(HATP)_2]^{4-}$ complexes, may imply protonation on either N(1) or on γ-phosphate, depending on the nature of M(II). It is possible that the two kinds of protonation do not appreciably differ with regard to the lattice energy, preserving the isomorphism of all the solids.

The C(6)–NH_2 length is 1.31(1) Å for the $[Mn(HATP)_2]^{4-}$ species, again in agreement with some double-bond character. The coplanarity of the NH_2 group with the adenine atoms is confirmed by the position of the two H atoms as determined with the analysis of the X-ray data.

II.6 The Role and Structure of the Aromatic Base

Most of the crystalline ATP-metal compounds contain an aromatic base, i.e., BIPY, PHEN, and DPA (see Fig. II.1.1). Inclusion of the base in the starting mixture of a divalent metal salt and Na_2H_2ATP

proved to be fruitful in obtaining crystalline materials. The BIPY or PHEN bases act as bidentate ligands for the Zn(II) and Cu(II) metal ions.[7,10] The nitrogen atoms occupy two equatorial positions and are *trans* to the γ- and β-phosphate oxygen donors. The four M–N distances average 2.14(4) and 2.01(1) Å for $[Zn(H_2ATP)\cdot(BIPY)]_2\cdot 4H_2O$[7] and $[Cu(H_2ATP)(PHEN)]_2\cdot 7H_2O$,[10] respectively, which are normal values for Zn(II)– and Cu(II)–N(pyridine) bond lengths.[17,19] The atoms of the PHEN systems are almost coplanar (with a maximum deviation of 0.09 Å) for both the molecules.

The DPA base does not act as ligand in the crystals containing the molecules of ATP bound to metal ions such as Mg(II), Ca(II), Mn(II), Co(II), Zn(II), and Cd(II). The DPA molecules were protonated in the ATP-metal compounds as opposed to the BIPY and PHEN bases. This can be due to the competition between the protons and metal ions towards the base which favors H^+ over some metal cations for DPA. It must be pointed out that pK_a values are 4.47,[32] 4.98,[32] and 7.14[33] for $HBIPY^+$, $HPHEN^+$ and $HDPA^+$, respectively. However, lattice energies, too, should play important roles in forming the solid species.

Structural studies of ternary complexes of Cu(II) ion with nucleotides and DPA show that the metal center is coordinated to the nitrogen atoms of the base.[34–37]

II.7 Stacking Interaction

Stacking interactions involving the adenine system and eventually the molecules of the second base play a prominent role in determining the stability of the crystal lattices of all the ATP-metal compounds. The dimers of $Na_2H_2ATP\cdot 3H_2O$[2,5a] are interleaved to produce *stacking interactions* between almost parallel adenine planes (Fig. II.7.1).[2] The mode of *stacking* shows minor changes upon dehydration to $Na_2H_2ATP\cdot 2H_2O$.[5a]

The angle between a pair of closest planes is about 179.3(4)° and 178.3(5)° for $Na_2H_2ATP\cdot 3H_2O$[5a] and $Na_2H_2ATP\cdot 2H_2O$,[5a] respectively; the average separation between the planes is 3.4 Å.[5a] The overlap is large and an approximate potential energy calculation[2] confirms that it corresponds to a minimum for inosine and guan-

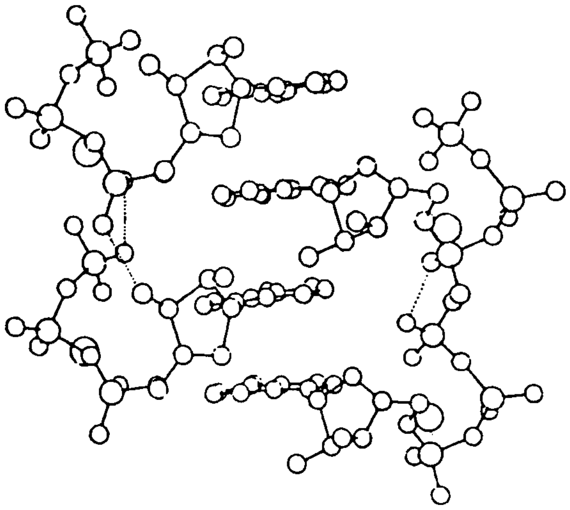

FIGURE II.7.1 View of the interleaved bases stacked in the crystallographic c direction for the disodium salt of ATP (from Ref. 2, with permission).

osine dihydrate. The *stacking interactions* are supported by H-bonds involving the stacked bases.

BIPY···adenine and BIPY···BIPY *stacking interactions* were found for the $[Zn(H_2ATP)(BIPY)]_2 \cdot 4H_2O^7$ complex. Adenine···adenine interactions are not present. The intramolecular BIPY···adenine interaction involves the five-membered ring of adenine, while the intermolecular interactions involve mostly the six-membered ring. The angles between the rings involved in the intramolecular and intermolecular *stacking interactions* range from 4 to 13°.

Intramolecular stacking interactions between the adenine system and the PHEN ligand are found for the $[Cu(H_2ATP)(PHEN)]_2 \cdot 7H_2O^{10}$ compound. The overlap involves only the imidazole ring of the adenine system. The closest contact involves a C(8) and a carbon atom of the PHEN ligand (3.32 Å). Dihedral angles between aromatic stacked rings are about 6°.

The *stacking interactions* for the $[M(HATP)_2][M_{1-q}M'_q(H_2O)_6] \cdot 2(HDPA) \cdot nH_2O$ compounds involve the adenine systems and both the $HDPA^+$ molecules (Fig. II.7.2). The two paired adenine

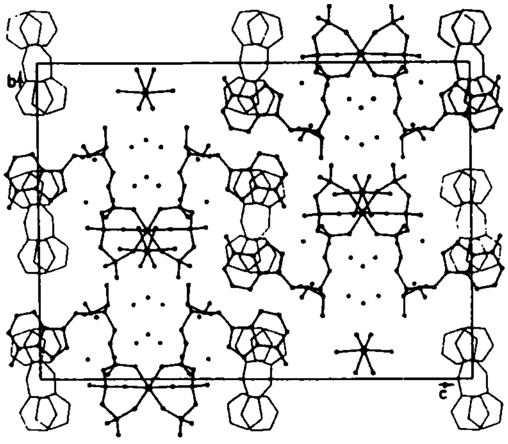

FIGURE II.7.2 Packing diagram of $[Mn(HATP)_2][Mn(H_2O)_6]\cdot 2(HADP)\cdot 12H_2O$ (from Ref. 14).

moieties sandwich both the $HDPA^+$ molecules, which are stacked with respect to each other. Both the pyridyl rings are involved in the $HDPA^+ \cdots HDPA^+$ as well as in the $HDPA^+ \cdots$adenine interactions. The overlap is large and the closest contact is 3.37 Å.

II.8 The Role of $[M(H_2O)_6]^{2+}$ Cations in the $[M(HATP)_2]$ $[M_{1-q}M'_q(H_2O)_6]\cdot 2(HDPA)\cdot nH_2O$ Compounds

The $[M(H_2O)_6]^{2+}$ cations have a distorted octahedral geometry. The coordinated water molecules are involved in H-*bonds* to the triphosphate chain oxygen atoms. The $[M(HATP)_2]^{4-}$ units[13-16] are sandwiched between $[M(H_2O)_6]^{2+}$ cations. The ***hexa-aqua*** species stabilize in this way the highly charged $[M(HATP)_2]^{4-}$ complexes. Large deviations from octahedral symmetry have been found for the $[Mg(H_2O)_6]^{2+}$ and $[Ca(H_2O)_6]^{2+}$ cations.[13,16]

The structures of the ATP-mixed metal compounds reveal that *alkaline earth* metal ions occupy preferentially the $[M(H_2O)_6]^{2+}$ sites while the *d-block* ions link to ATP, when the two metals are in a molar ratio of 1 in the crystal. As the six water molecules can be located in a more flexible way around *alkaline earth* than around *d-block* metal cations, the $[Mg(H_2O)_6]^{2+}$ and $[Ca(H_2O)_6]^{2+}$ cations are presumably suitable to give the strongest H-*bonds* to the triphosphate chain.

The role of a second metal ion interacting with ATP is invoked for phosphate transfer reactions.[38] Proposed mechanistic steps for the polyphosphate hydrolysis are: (1) coordination of the metal ions to the β and γ groups to reduce the nucleophilicity of the polyphosphate; (2) coordination of a second metal ion, having *cis* coordination positions available, to the γ group; (3) hydrolytic attack by the *cis*-hydroxide on the polyphosphate chain.

II.9 Hydrogen Bonds

H-*bonds* between β-phosphate oxygen atoms and the NH_2 groups of the two ATP molecules of $Na_2H_2ATP \cdot 3H_2O$ play an important role in stabilizing the dimer itself.[2,5a] Moreover, the dimeric units are held together mostly by H-*bonds* involving oxygen atoms from the phosphate chain and the sugar moiety. Interleaving columns of dimers are linked by H-*bonds* involving N(1) and γ-phosphate oxygen atoms. Water molecules are close to some of the Na^+ cations, completing their coordination spheres. Furthermore, these water molecules are involved in the hydrogen bonding network. There are some kinds of channels which contain the free water molecules. Hydrophilic channels are found in all structures of ATP-metal compounds. The channels are usually relatively open so that the H_2O molecules can easily move and even effloresce, causing some alteration in the strength of the bonds between "*blocks*." Some of the water molecules of $Na_2H_2ATP \cdot 3H_2O$[2,5a] interact, via H-*bonds*, with the phosphate oxygen atoms and with the hydroxyl groups of the riboses. They are lost during the transition to $Na_2H_2ATP \cdot 2H_2O$[5a]; this loss is related to the conformational changes of the ribose groups.[5a] A series of other changes in the H-*bond* network follows the dehydration phenomenon.

Intermolecular H-*bonds* in $[Zn(H_2ATP)(BIPY)]_2 \cdot 4H_2O$[7] involve the free oxygen atom of the α-phosphate, the N(1) atom of adenine and the free oxygen atom of the γ-phosphate. Dimers related by the screw axis are linked via H-*bonds* involving the ribose and phosphate oxygens.

All the oxygen atoms of the triphosphate chain of $[M(HATP)_2][M_{1-q}M'_q(H_2O)_6] \cdot 2(HDPA) \cdot nH_2O$ compounds,[13-16] which are not involved in the P–O–P bridges, participate in the hydrogen bonding scheme. The N(1) nitrogen atom is involved in an intermolecular H-*bond* with one of the free oxygen atoms from the γ-phosphate. The NH_2 and N(7) groups are involved in H-*bonds* that pair two adenine bases symmetrically related by a two-fold axis.

The free water molecules are located in the channels around the phosphate chains and the ribose rings. They stabilize the $[M(HATP)_2]^{4-}$ unit by linking the two phosphate chains via H-*bonds*.

III. ADP-METAL COMPOUNDS

The ADP-metal compounds studied by X-ray diffraction are listed in Table III.1.

III.1 Synthesis of ADP-Metal Compounds

Thin needles of $KH_2ADP \cdot 2H_2O$ were prepared by slow evaporation of a water/ethanol solution (pH 6.3) of the substance at 280 K.[39] The structure was refined down to *R* 6.2%. Smaller crystals were obtained at pH 4 from a water/ethanol solution.[40]

$RbH_2ADP \cdot H_2O$ was crystallized (as poor quality needles) from a water/ethanol solution of H_3ADP and RbBr (1:1 molar ratio). The pH was fixed at 5.5 by using Tris buffer, and the solution temperature was maintained at 5°C. The structure was refined to an *R* index of 11.9%.[42]

$[Cu_4(HADP)_2(BIPY)_4(H_2O)_2(NO_3)_2] \cdot (NO_3)_2$ was prepared from a mixture of copper nitrate, BIPY, NaH_2ADP (molar ratio 1:1:1) and water. The pH was adjusted to 4.0 and the solution heated up to 80°C. Small crystals formed in a period of 3–4 weeks as plates. The structure was refined to *R* 15.5%.[10]

III.2 The Pyrophosphate Group

The backbone P–O bond lengths and the P–O–P bond angles for ADP-metal compounds are reported in Table III.2.1. It should be noted that the P(α)–O($\alpha\beta$) bond length is higher than the O($\alpha\beta$)–P(β) distance for the $KH_2ADP \cdot 2H_2O$,[39] $K_2HUDP \cdot 3H_2O$,[46] and

TABLE III.1

ADP-metal compounds studied with X-ray diffraction methods[a]

Compound	Preparation	Space Group	R_F%	Ref.
$KH_2ADP\cdot 2H_2O$	water/ethanol	$P2_12_12$	6.2	39
	water/ethanol	$P2_12_12$	9.3[b]	40
$RbH_2ADP\cdot H_2O$	water/ethanol	$P2_12_12$	11.9	41, 42
$[Cu_4(HADP)_2(BIPY)_4$-$(H_2O)_2(NO_3)_2]\cdot(NO_3)_2$	water, pH 4	$P2_1$	15.5	10
$H_3ADP\cdot 3H_2O$			7.8	43
Tris-$H_2ADP\cdot 2H_2O$	water, Tris buffered/ acetone	$P2_1$	4.7	44
$H_3CDP\cdot H_2O$	water/acetone/ethanol	C2	6.3	45
$NaHCDPC\cdot 5H_2O$	water/acetone/ethanol	$P2_12_12_1$	9.1	45
$K_2HUDP\cdot 3H_2O$	water/ethanol	$P2_12_12_1$	5.9	46
NDP	dimethyl sulfoxide/ ethanol/pyridine	$P2_1/c$	6.5	47
$TDP\cdot HCl$	water/ethanol	$P2_1/c$	3.7	48
$LiNAD\cdot 2H_2O$	water, pH 4/methanol	$P2_12_12_1$	10.0	49

[a] $H_3ADP\cdot 3H_2O$, Tris-$H_2ADP\cdot 2H_2O$ (Tris = $(HOCH_2)_3(CH_3)N$), $H_3CDP\cdot H_2O$ (CDP = cytidine 5′-diphosphate), $NaHCDPC\cdot 5H_2O$ (CDPC = cytidine 5′-diphosphocholine), $K_2HUDP\cdot 3H_2O$ (UDP = uridine 5′-diphosphate), NDP (= P^1, P^2-di-β-naphthyl pyrophosphate dicyclohexylammonium salt), $TDP\cdot HCl$ (TDP = thiamine pyrophosphate) and $LiNAD\cdot 2H_2O$ (NAD = nicotinamide adenine dinucleotide) are also included for comparison.

[b] Rw value.

$TDP\cdot HCl$[48] compounds, and possibly for the $[Cu_4(HADP)_2(BIPY)_4(H_2O)_2(NO_3)_2]\cdot(NO_3)_2$[10] complex (on the other hand, the terminal P–O backbone linkage is the longest for most of the ATP derivatives). The P–O–P angle of 131.3(4)° for $KH_2ADP\cdot 2H_2O$ is normal when compared with other ATP- and ADP-metal compounds.

The pyrophosphate oxygen atoms of $KH_2ADP\cdot 2H_2O$[39] exhibit the usual staggered conformations about the P(α) ··· P(β) axis (Fig. III.2.1). The metal ion is coordinated to two oxygen atoms from the β-phosphate group and to an oxygen atom from the α-phosphate group. The K–O bond distances are 3.238(8) and 2.953(8), and 2.767(8) Å for the β-phosphate and α-phosphate groups respectively. The short K–O(α) bonding interaction has to be compared with the long P(α)–O(αβ) bond distance. It should be noted that the structure of $K_2HUDP\cdot 3H_2O$[46] shows a similar feature for the P–O backbone distance and the metal ions coordinate to the

TABLE III.2.1

Backbone pyrophosphate geometrical parameters for the ADP-metal compounds. Data relevant to other diphosphate compounds are also listed

Compound	P(α)-O(αβ)/Å	P(β)-O(αβ)/Å	P-O-P/°
$KH_2ADP \cdot 2H_2O$	1.626(8)	1.609(8)	131.3(4)
$RbH_2ADP \cdot H_2O$	1.54(2)	1.64(2)	135(1)
$[Cu_4(HADP)_2\text{-}(BIPY)_4(H_2O)_2\text{-}(NO_3)_2] \cdot (NO_3)_2$	1.69(6)	1.58(6)	132(4)
	1.57(4)	1.56(4)	140(4)
$Tris\text{-}H_2ADP \cdot 2H_2O$	1.585(6)	1.627(5)	130.5(3)
$H_3CDP \cdot H_2O$	1.58(1)	1.62(1)	127.8(5)
$NaHCDPC \cdot 5H_2O$	1.60(1)	1.64(1)	131.7(8)
$K_2HUDP \cdot 3H_2O$	1.617(8)	1.566(7)	129.6(5)
	1.597(9)	1.572(9)	133.7(5)
NDP[a]	1.593(4)	1.611(4)	134.2(2)
TDP·HCl	1.602(2)	1.583(2)	133.6(1)
$LiNAD \cdot 2H_2O$[a]	1.56(1)	1.66(1)	133(1)

[a]Both phosphate groups are esterified.

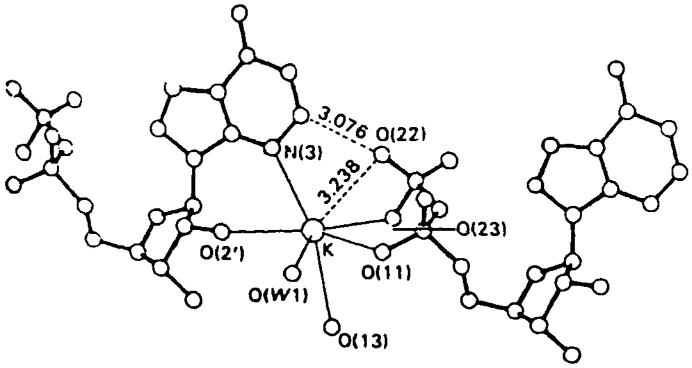

FIGURE III.2.1 Coordination sphere around the K^+ cation of $KH_2ADP \cdot 2H_2O$ (from Ref. 39, with permission).

α- and β-phosphate groups. The K^+ ion of $KH_2ADP \cdot 2H_2O$[39] coordinates also to a second nucleotide through the N(3) and O(2') atoms, and to a third ADP molecule via a O(α) atom; finally the coordination sphere is completed by a water molecule. There is no intramolecular metal bridge between the adenine base and the phosphate groups.

The structure of $RbH_2ADP \cdot H_2O$[42] is isostructural with that of $KH_2ADP \cdot 2H_2O$.[39] The two structures differ by a water molecule that bridges two K^+ ions in $KH_2ADP \cdot 2H_2O$[39]; this water molecule was not found in the Rb^+ salt. The pyrophosphate moiety of $RbH_2ADP \cdot H_2O$[42] shows a relevant difference of 0.1 Å (Table III.2.1) for the P(α)–O(αβ) and P(β)–O(αβ) bond distances. The order of lengthening of the P–O backbone linkages is reversed when compared with the K^+ salt. However, the poorer accuracy of the structure of the Rb derivative makes this result less significant, even though the influence of metal ion dimension cannot be excluded. The P–O–P bond angle is 135(1)°.

The poor quality of the data makes impossible a detailed discussion of the structure of $[Cu_4(HADP)_2(BIPY)_4(H_2O)_2(NO_3)_2] \cdot (NO_3)_2$[10] (Fig. III.2.2). The complex displays two Cu(II) ions, with bidentate equatorial coordination involving α- and β-phosphate oxygen atoms of ADP molecules. The coordination geometry of these Cu(II) centers is square pyramidal. Two of the basal sites are occupied by BIPY nitrogen atoms. The metal ions shift slightly towards the axial ligand, which is provided by a β-phosphate oxy-

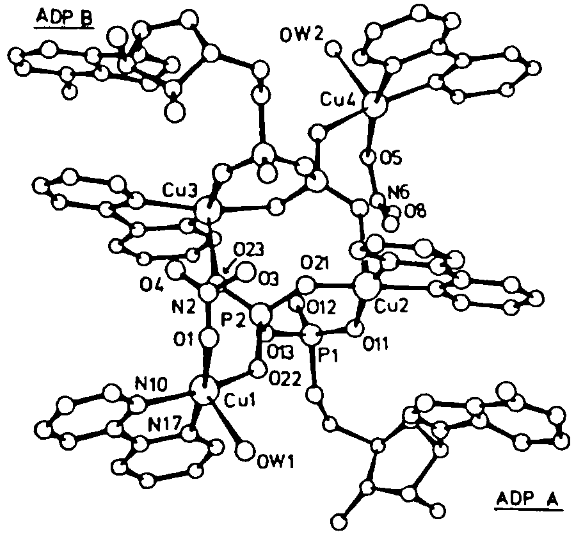

FIGURE III.2.2 Structure of the $[Cu_4(HADP)_2(BIPY)_4(H_2O)_2(NO_3)_2]^{2+}$ complex (from Ref. 10, with permission).

gen atom. The basal Cu–O bond distances average 1.92(4) Å, while the axial ones average 2.29(4) Å. The other two Cu(II) ions show a monodentate coordination by the β-phosphate oxygen atoms. However, these Cu(II) centers also have a square pyramidal geometry completed by two BIPY nitrogen atoms and a nitrate oxygen atom in the equatorial plane. The axial position is occupied by a water molecule. All three peripheral oxygen atoms of the β-phosphate groups are coordinated to three different Cu(II) ions.

The conformation of the pyrophosphate chain is revealed by the torsion angles. The C(4′)–C(5′)–O(5′)–P(α) torsion angle in $KH_2ADP \cdot 2H_2O^{39}$ and $RbH_2ADP \cdot H_2O^{42}$ (144.6(5) and 147(3)°, respectively) shows a large deviation from the *trans* conformation and can be described as +*ac*. The C(5′)–O(5′)–P(α)–O(αβ) torsion angle for $KH_2ADP \cdot 2H_2O^{39}$ is −63.6(5)°, so the conformation around O(5′)–P(α) can be described as *gauche*⁻. This feature is characteristic of the nucleic acids with right-handed helical conformation,[22] and of most of the ATP molecules. The O(5′)–P(α)–O–P(β) torsion angle (157.3(5)°) shows some deviation from the ideal *trans* conformation; it can be described as +*ap*.

III.3 Chelate Ring Conformation and Chirality of Coordination

The Q_T parameter[23] of the six-membered chelate ring of $KH_2ADP \cdot 2H_2O^{39}$ (taking into account only the strongest metal coordination to the β-phosphate group) is 0.93, and corresponds to a distorted chair conformation. The chirality of the chelate ring can be designated as Δ.[24] The Q_T parameter for the chelate ring of $RbH_2ADP \cdot H_2O^{42}$ is 0.91.

The Q_T parameters relevant to the chelate rings involving the two ADP molecules of $[Cu_4(HADP)_2(BIPY)_4(H_2O)_2(NO_3)_2](NO_3)_2{}^{10}$ are 0.45 and 0.21, while the chirality of coordination is Δ and Λ, respectively.

III.4 The Ribose Group

Some parameters that define the ribose ring conformation are listed in Table III.4.1 (see Fig. II.4.1). The conformation of the ribose rings for the $KH_2ADP \cdot 2H_2O^{39}$ and $RbH_2ADP \cdot H_2O^{42}$ compounds is C(2′)-*endo*. The O(2′) atom is coordinated to the metal ions in both the K^+ and Rb^+ salts of ADP.

TABLE III.4.1

Some torsion angles (°) and phase angle of pseudorotation of the ribose (P) for the ADP-metal compounds. Data relevant to $K_2HUDP \cdot 3H_2O$ are included for comparison

Compound	χ	ψ_{oc}	Conformation	P^a
$KH_2ADP \cdot 2H_2O$	32(1)	58(1)	C(2′)-*endo*	163
$RbH_2ADP \cdot H_2O$	40(3)	57(3)	C(2′)-*endo*	163
$[Cu_4(HADP)_2(BIPY)_4(H_2O)_2$-	47(5)	68(5)		
$(NO_3)_2] \cdot (NO_3)_2$	3(5)	72(5)		
$KHUDP \cdot 3H_2O$	45(1)	52(1)	C(2′)-*endo*	157
	41(1)	54(1)	C(2′)-*endo*	165

[a] See note to Table II.4.1.

III.5 The Adenine Group

The bond lengths and bond angles of the adenine system of $KH_2ADP \cdot 2H_2O^{39}$ are in agreement with the values found for the ATP-metal compounds. The C(2)–N(1)–C(6) bond angle of 124.6(7)° is in agreement with protonation of N(1) on the basis of the Singh rule.[31] The C(2)–N(1)–C(6) bond angle of $RbH_2ADP \cdot H_2O^{42}$ is 121(2)°. The C(6)–N(6) bond distance is 1.293(13) and 1.35(3) Å in the K^+ and Rb^+ salt, respectively. The conformation around the N(9)–C(1′) bond can be described as *anti* for the K^+ and Rb^+ salt (χ = 32(1) and 40(3)°, respectively). It is noteworthy that the N(3) nitrogen atom is coordinated to both K^+ and Rb^+, a rather uncommon feature for adenine nucleotides.

The N(7) nitrogen atom is not coordinated to the metal ion. However, the N(7) atom is involved in an intermolecular H-*bond* to the β-phosphate group. N(1) and NH_2 also interact intermolecularly with β-phosphate oxygen atoms via H-*bonds* (Fig. III.5.1).

The structure of $[Cu_4(HADP)_2(BIPY)_4(H_2O)_2(NO_3)_2]\ (NO_3)_2{}^{10}$ reveals that N(1) atoms are presumably protonated, as all the oxygen atoms of the β-phosphate group are coordinated to Cu(II) ions. The nitrogen atoms are not involved in any interaction with the metal ions. The N(6) and N(7) atoms are connected via H-*bonds* that pair two bases related by a translation along the **a** axis. The conformation of the adenine base around the N(9)–C(1′) bond is *anti* for both the nucleotide molecules, the χ angles being 47° and 3°, respectively.

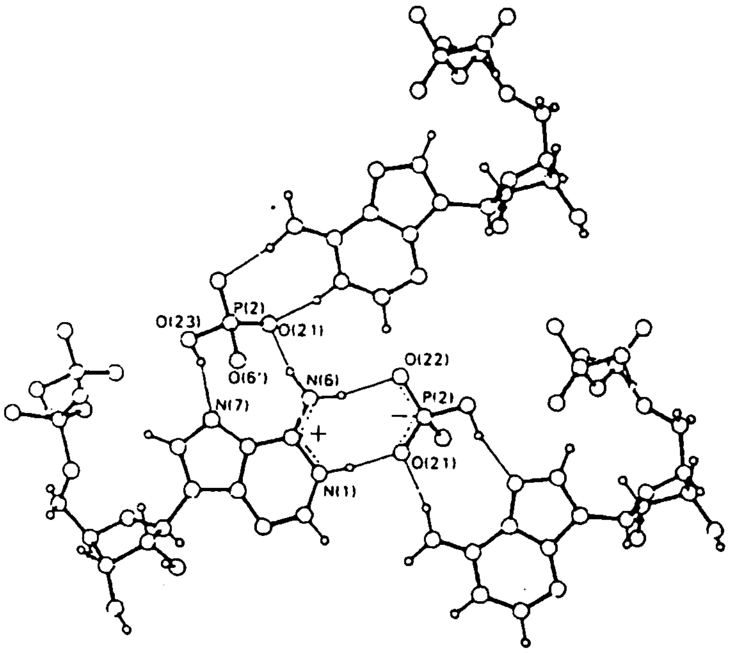

FIGURE III.5.1 View of the base··· phosphate pairing interactions in $KH_2ADP\cdot 2H_2O$ (from Ref. 39, with permission).

III.6 The Stacking Interaction and the Role and Structure of BIPY Base

For the $KH_2ADP\cdot 2H_2O$[39] and $RbH_2ADP\cdot H_2O$[42] compounds, there is an absence of base *stacking*. However, an intermolecular sugar··· adenine interaction exists. The O(4′) oxygen atom of the sugar lies under the six-membered ring of the neighboring adenine (Fig. III.6.1). Short interatomic contacts exist between O(4′) and N(1), C(6), C(2), C(4) and C(5) atoms. This kind of interaction is sometimes observed in nucleosides and nucleotides having a protonated base[50]; however, it was not found for other ATP- and ADP-metal compounds.

The BIPY base plays two important roles in the $[Cu_4(HADP)_2(BIPY)_4(H_2O)_2(NO_3)_2]\,(NO_3)_2$[10] complex: (1) it acts as a chelating ligand for all four metal centers; (2) it is involved

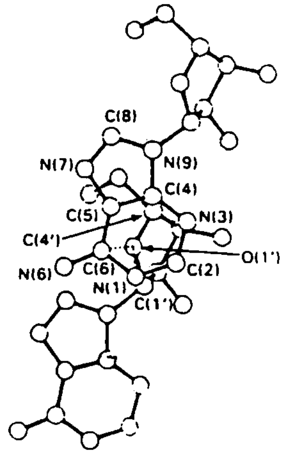

FIGURE III.6.1 The diagram shows the overlapping of the adenine system on the neighboring ribose ring found in $KH_2ADP \cdot 2H_2O$ (from Ref. 39, with permission).

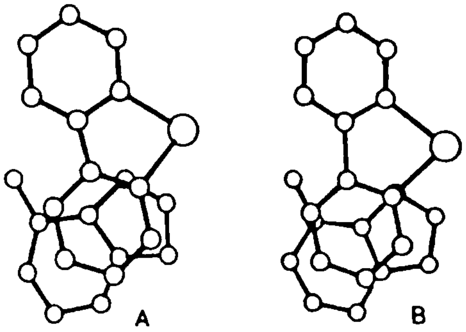

FIGURE III.6.2 Intramolecular stacking interaction between the adenine and BIPY systems of the $[Cu_4(HADP)_2(BIPY)_4(H_2O)_2(NO_3)_2]^{2+}$ complex (from Ref. 10, with permission).

in intramolecular *stacking interactions* with the adenine system (Fig. III.6.2). The dihedral angles between the BIPY and adenine systems of the same complex molecule are about 5°; one of the rings of the BIPY ligand overlaps large regions of both six- and five-membered rings of adenine. The closest interatomic contact is 3.2 Å.

IV. CONCLUSION

It is evident that ATP-metal compounds are useful models for biological systems. The study of these species, through X-ray diffraction, allows a high resolution determination of the atomic positions which is not obtainable with any other technique in solution, or even in the solid state for enzyme/M/ATP systems. Inasmuch as it has been shown that similar coordination patterns were found for model compounds[13,14,16] and some enzyme/M/ATP complexes (Ref. 1o and references therein), the structures of M-ATP compounds can reasonably be used to fit the electron density maps derived from X-ray analysis of enzyme-containing systems as well as in interpreting the spectroscopic and kinetic data of biological complexes. Therefore more work on nucleoside triphosphate–metal compounds must be carried out.

Among other topics, the following ones, in my opinion, should be taken into account: (a) the synthesis and X-ray characterization of metal complexes with nucleotide and amino acids or oligopeptides; (b) the synthesis and X-ray characterization of metal complexes containing amino acid, nucleoside triphosphate and nucleoside monophosphate; amino acid, nucleoside diphosphate and orthophosphate; amino acid, nucleoside monophosphate and pyrophosphate; phosphorylated amino acid and nucleoside diphosphate; (c) the synthesis and X-ray characterization of bi-/polymetallic complexes with nucleoside triphosphates; (d) the in-depth investigation of hydration phenomena for the solid state of metal–nucleotide complexes; and (e) the development of well refined force-fields suitable for molecular mechanics calculations on metal–nucleotide complexes.

Data collected from compounds mentioned in (a) will give important insights into the nature of interactions in the substrate (S) bridge (E–S–M), metal bridge (E–M–S), and enzyme (E) bridge (M–E–S or $\overline{\text{E–M–S}}$) types of coordination scheme (see Ref. 1c and references therein). Compounds such as those indicated in (b) should give useful information about the mechanism of the catalytic phosphotransfer and nucleotidyl transfer reactions as well as on the stereochemistry of the intermediate of reaction. In fact, the question whether substitution at phosphorous proceeds via a single-displacement or a double-displacement pathway, and whether it is an associative or dissociative process[1d,1o,51] has prompted a large number of investigations and still has no suitable answers for many processes. Compounds such as those mentioned in (c) should shed light on the catalytic role of two metal centers in reactions involving at least two metal ions per active site (see for example Ref. 1f). Studies such as those mentioned in (d) should reveal the dynamic aspects of nucleotide-metal structures and provide a sound basis for theoretical models of the solution phase.[5a] Finally, a large number of X-ray structures of nucleoside triphosphate-metal complexes, together with spectroscopic data from solid and solution phases, will allow the development of rigorous force-fields for molecular mechanics calculations (e). The combination of this kind of computation with nuclear magnetic resonance experiments,[52] in turn, will be of increasing importance in gaining insights about the solution structures being elucidated as a consequence of advances in instrumentation, computers and computational methods.

Regarding the formation of good quality single crystals, the data reviewed here indicate that the pH of the mother liquor plays a prominent role. Owing to the presence of a high number of basic sites on the nucleotides, the distribution diagrams of the metal species are strongly dependent on pH. Potentiometric and/or spectrophotometric titrations on the chosen systems should therefore be carried out to produce suitable distribution diagrams as a function of pH and molar ratio of components.

Furthermore, the presence of metal ions often increases the rate of hydrolysis of the nucleoside triphosphate and this phenomenon is dependent on pH. Since crystallization procedures usually require long times (from some hours to some weeks) and starting solutions often must be dilute, the pH (and temperature) should be adjusted so as to decrease decomposition of the nucleotide molecule. Such precautions and systematic investigation of crystallization procedures may overcome the limitations imposed by the relatively few relevant ATP structures.

References

1. (a) A. L. Lehninger, *Principles of Biochemistry* (Worth Publishers, Inc., New York, 1982);

(b) J. D. Watson, N. H. Hopkins, J. W. Roberts, J. A. Steitz and A. M. Weiner, *Molecular Biology of the Gene* (The Benjamin-Cummings Publishing Company, Inc., Menlo Park, California, 1987), Vol. 1, fourth edition;
(c) H. Yan and M.-D. Tsai, Biochemistry **30**, 5539 (1991);
(d) J. P. Jones, P. M. Weiss and W. W. Cleland, Biochemistry **30**, 3634 (1991);
(e) C. E. Karkaria, R. F. Steiner and B. P. Rosen, Biochemistry **30**, 2625 (1991);
(f) L. M. Abell and J. J. Villafranca, Biochemistry **30**, 1413 (1991);
(g) P. S. Leventhal and P. J. Bertics, Biochemistry **30**, 1385 (1991);
(h) J. Mendell-Hartvig and R. A. Capaldi, Biochemistry **30**, 1278 (1991);
(i) J. J. Neitzel, W. R. G. Dostmann and S. S. Taylor, Biochemistry **30**, 733 (1991);
(j) H. G. Wood and J. E. Clark, Ann. Rev. Biochem. **57**, 235 (1988);
(k) Y. Hatefi, Ann. Rev. Biochem. **54**, 1015 (1985);
(l) P. V. Vignais and J. Lunardi, Ann. Rev. Biochem. **54**, 977 (1985);
(m) S. P. Bessman and C. L. Carpenter, Ann. Rev. Biochem. **54**, 831 (1985);
(n) H. S. Penefsky and R. L. Cross, Adv. in Enzymology **64**, 173 (1991);
(o) P. A. Frey, Adv. in Enzymology **62**, 119 (1989);
(p) S. Fleisher and B. Fleisher (Eds.), Methods in Enzymology **156** (1988);
(q) T. Hunter and B. M. Sefton (Eds.), Methods in Enzymology **200** (1991);
(r) T. Hunter and B. M. Sefton (Eds.), Methods in Enzymology **201** (1991);
(s) A. Babloyantz, *Molecules, Dynamics & Life, an Introduction to Self-Organization of Matter*, eds. I. Prigogine and G. Nicolis (J. Wiley & Sons, New York, 1986), Vol. IV in the series: Non-equilibrium Problems in the Physical Sciences and Biology;
(t) R. J. P. Williams, J. Chem. Soc., Dalton Trans. **1991**, 539;
(u) M. D. Reily, T. W. Hambley and L. G. Marzilli, J. Am. Chem. Soc. **110**, 2999 (1980);
(v) G. Liang and H. Sigel, Inorg. Chem. **29**, 3631 (1990);
(w) R. B. Martin, Met. Ions Biol. Syst. **23**, 315 (1988);
(x) H. Sigel, R. Tribolet, R. Malini-Balakrishnan and R. B. Martin, Inorg. Chem. **26**, 2149 (1987);
(y) L. G. Marzilli, T. J. Kistenmacher and G. L. Eichhorn, Perspectives on Metals in Biology, Met. Ions in Biology **1**, 179 (1980);
(z) J. K. Barton and S. J. Lippard, Met. Ions in Biology **1**, 31 (1980);
(ia) B. de Castro, T. J. Kistenmacher and L. G. Marzilli, in *Trace Elements in the Pathogenesis and Treatment of Inflammatory Conditions*, eds. K. D. Rainsford, K. Brune and M. W. Whitehouse, Agents and Actions, Basel, 1981;
(ib) L. G. Marzilli, in *Metal Ions in Genetic Information Transfer*, eds. G. L. Eichhorn and L. G. Marzilli (Elsevier/North-Holland, New York, 1981), **3**;
(ic) S. E. Sherman and S. J. Lippard, Chem. Rev. **87**, 1153 (1987);
(id) P. Köpf-Maier and H. Köpf, Chem. Rev. **87**, 1137 (1987);
(ie) J. Reedijk, A. M. J. Fichtinger-Schepman, A. T. van Oosterom and P. van de Putte, Struct. Bonding **67**, 53 (1987);
(if) R. B. Martin and H. Sigel, Comments Inorg. Chem. **6**, 285 (1988);
(ig) B. Lippert, Prog. Inorg. Chem. **37**, 1 (1989);
(ih) J. Rubin and D. M. Blow, J. Mol. Biol. **145**, 489 (1981);
(ii) R. D. Banks, C. C. F. Blake, P. R. Evans, R. Haser, D. W. Rice, G. W. Hardy, M. Merrett and A. W. Phillips, Nature **279**, 773 (1979);
(ij) C. Monteilhet and D. M. Blow, J. Mol. Biol. **122**, 407 (1978);
(ik) M. Shoham and T. A. Steitz, J. Mol. Biol. **140**, 1 (1980).

2. O. Kennard, N. W. Isaacs, W. D. S. Motherwell, J. C. Coppola, D. L. Wamp-

ler, A. C. Larson and D. G. Watson, Proc. R. Soc., London, Ser. A **325**, 401 (1971).

3. O. Kennard, N. W. Isaacs, J. C. Coppola, A. J. Kirby, S. Warren, W. D. Motherwell, D. G. Watson, D. L. Wampler, D. H. Chenery, A. C. Larson, K. A. Kerr and L. Riva di Sanseverino, Nature **225**, 333 (1970).
4. A. C. Larson, Acta Crystallogr., Sect. B **34**, 3601 (1978).
5. (a) Y. Sugawara, N. Kamiya, H. Iwasaki, T. Ito and Y. Satow, J. Am. Chem. Soc. **113**, 5440 (1991);
   (b) Y. Sugawara and H. Iwasaki, Acta Crystallogr., Sect. A **40**, C68 (1984).
6. P. Orioli, R. Cini, D. Donati and S. Mangani, Nature (London) **283**, 691 (1980).
7. P. Orioli, R. Cini, D. Donati and S. Mangani, J. Am. Chem. Soc. **103**, 4446 (1981).
8. R. Cini and P. Orioli, J. Inorg. Biochem. **14**, 95 (1981).
9. W. S. Sheldrick, Angew. Chem. **93**, 473 (1981).
10. W. S. Sheldrick, Z. Naturforsch. **37b**, 863 (1982).
11. R. Cini, A. Cinquantini, M. C. Burla, A. Nunzi, G. Polidori and P. F. Zanazzi, Chim. Ind. (Milan) **64**, 826 (1982).
12. R. Cini, M. Sabat, M. Sundaralingam, M. C. Burla, A. Nunzi, G. Polidori and P. F. Zanazzi, J. Biomol. Struct. Dyn. **1**, 633 (1983).
13. R. Cini, M. C. Burla, A. Nunzi, G. Polidori and P. F. Zanazzi, J. Chem. Soc., Dalton Trans. **1984**, 2467.
14. M. Sabat, R. Cini, T. Haromy and M. Sundaralingam, Biochemistry **24**, 7827 (1985).
15. R. Cini, M. Sabat and M. Sundaralingam, unpublished results.
16. R. Cini and L. G. Marzilli, Inorg. Chem. **27**, 1855 (1988).
17. R. H. Prince, in *Comprehensive Coordination Chemistry*, ed. G. Wilkinson (Pergamon Press, Oxford, 1987), Vol. 5, Ch. 56.1.
18. R. J. P. Williams, in *Zinc in Human Biology*, ed. C. F. Mills (Springer-Verlag, Berlin, 1989).
19. B. J. Hathaway, in *Comprehensive Coordination Chemistry*, ed. G. Wilkinson (Pergamon Press, Oxford, 1987), Vol. 5, Ch. 53.
20. W. Saenger, *Principles of Nucleic Acid Structure* (Springer-Verlag, Berlin, 1984).
21. R. D. Shannon and C. T. Prewitt, Acta Crystallogr., Sect. B **26**, 1076 (1970).
22. M. Sundaralingam, Biopolymers **7**, 821 (1969).
23. D. Cremer and J. A. Pople, J. Am. Chem. Soc. **97**, 1354 (1975).
24. E. A. Merritt, M. Sundaralingam, R. D. Cornelius and W. Cleland, Biochemistry **17**, 3274 (1978).
25. (a) W. Saenger, Angew. Chem., Int. Ed. Engl. **12**, 591 (1973);
    (b) M. A. Viswamitra, B. S. Reddy, H.-Y. Lin and M. Sundarlingam, J. Am. Chem. Soc. **93**, 4565 (1971);
    (c) A. E. V. Aschemeier and A. Rich, J. Mol. Biol. **27**, 369 (1967).
26. C. Still, F. Mohamadi, N. G. J. Richards, W. C.. Guida, M. Lipton, R. Liskamp, G. Chang, T. Hendrickson, F. de Gunst and G. W. Hasel, *MacroModel V3.0*, Department of Chemistry, Columbia University, NY (1990).
27. (a) S. J. Weiner, P. A. Kollman, D. A. Case, U. C. Singh, C. Ghio, G. Alagona, S. Profeta, Jr. and P. Weiner, J. Am. Chem. Soc. **106**, 765 (1984);
    (b) S. J. Weiner, P. A. Kollman, D. T. Nguyen and D. A. Case, J. Comp. Chem. **7**, 230 (1986).
28. A. Bondi, J. Phys. Chem. **68**, 441 (1964).

29. A. I. Kitaigorodsky, *Molecular Crystals and Molecules* (Academic Press, London, 1973).
30. R. Taylor and O. Kennard, J. Am. Chem. Soc. **104**, 5063 (1982).
31. C. Singh, Acta Crystallogr. **19**, 861 (1965).
32. H. Irving and D. H. Miller, J. Chem. Soc. **1962**, 5222.
33. G. Anderegg, Helv. Chim. Acta **54**, 509 (1971).
34. B. E. Fischer and R. Bau, Inorg. Chem. **17**, 27 (1978).
35. R. W. Gellert, B. E. Fischer and R. Bau, Biochim. Biophys. Res. Commun. **88**, 1443 (1979).
36. G. Giorgi and R. Cini, Inorg. Chim. Acta **151**, 153 (1988).
37. F. Laschi, M. P. Picchi, C. Rossi and R. Cini, Inorg. Chim. Acta **135**, 215 (1987).
38. (a) G. P. Haight, Jr., Coord. Chem. Rev. **79**, 293 (1987);
    (b) H. Sigel, Pure Appl. Chem. **55**, 137 (1983).
39. P. Swaminathan and M. Sundaralingam, Acta Crystallogr., Sect. B **36**, 2590 (1980).
40. D. A. Adamiak and W. Saenger, Acta Crystallogr., Sect. B **36**, 2585 (1980).
41. A. Mueller and A. B. Deluke, Am. Cryst. Assoc. (Winter) **1971**, 26.
42. (a) M. A. Viswamitra, M. V. Hosur, Z. Shakked and O. Kennard, Cryst. Struct. Commun. **5**, 819 (1976);
    (b) M. A. Viswamitra, M. V. Hosur, Z. Shakked and O. Kennard, Nature (London) **262**, 234 (1976).
43. (a) M. V. Hosur and M. A. Viswamitra, Curr. Sci. **48**, 1027 (1979);
    (b) M. A. Viswamitra and M. W. Hosur, *Abstract of the 4th European Crystallographic Meeting, Oxford* (Cotswold Press Ltd., Oxford, 1977), p. 265.
44. Z. Shakked, M. A. Viswamitra and O. Kennard, Biochemistry **19**, 2567 (1980).
45. M. A. Viswamitra, T. P. Seshadri, M. L. Post and O. Kennard, Nature (London) **258**, 497 (1975).
46. M. A. Viswamitra, M. L. Post and O. Kennard, Acta Crystallogr., Sect. B **35**, 1089 (1979).
47. M. K. Wood, M. Sax and J. Pletcher, Acta Crystallogr., Sect. B **31**, 76 (1975).
48. (a) J. Pletcher and M. Sax, J. Am. Chem. Soc. **94**, 3998 (1972);
    (b) C. H. Carlisle and D. S. Cook, Acta Crystallogr., Sect. B **25**, 1359 (1969).
49. W. Saenger, B. S. Reddy, K. Mühelegger and G. Weinmann, Nature **267**, 225 (1977).
50. (a) C. E. Bugg, J. Thomas, M. Sundaralingam and S. T. Rao, Biopolymers, **10**, 175 (1971);
    (b) M. Sundaralingam, Biopolymers **6**, 189 (1968).
51. R. J. Leatherbarrow, A. R. Fersht and G. Winter, Proc. Natl. Acad. Sci. (USA) **82**, 7840 (1985).
52. R. Cini, G. Giorgi, F. Laschi, C. Rossi and L. G. Marzilli, J. Biomol. Struct. Dyn. **7**, 859 (1990).